2016 International Symposium on Nonlinear Theory and Its Applications,
NOLTA2016, Yugawara, Japan, November 27th-30th, 2016

Modeling and Stabilization of the Novel Quadrotor with Tilting Propeller

Takumi Fukuda,† Akinori Sakaguchi,† Takashi Takimoto,‡ and Toshimitu Ushio†

†Graduate School of Engineering Science, Osaka University
1–3 Machikaneyama, Toyonaka, Osaka, 560-8531 Japan
‡Department of Creative Engineering, National Institute of Technology, Kitakyushu College
5–20–1 Shii, Kokuraminamiku, Kitakyushu, Fukuoka, 802-0985 Japan
Email: fukuda, sakaguchi@hopf.sys.es.osaka-u.ac.jp, takashi@kct.ac.jp, ushio@sys.es.osaka-u.ac.jp

Abstract—The quadrotors are useful for periodic inspection of tunnels and bridges. However, the conventional quadrotor has a problem such that it is impossible to control the rotational motion and the translational motion independently. Therefore, if the camera is attached on the bottom of the quadrotor, it is difficult to observe its upward direction. In this paper, we develop a novel quadrotor that has a link to tilt its propellers. By increasing the degree of freedom of the quadrotor, we resolve the problems described above. And we derive a model of the developed quadrotor. Then, we consider a PID controller for the stabilization of the quadrotor at a specified hovering state. We derive gain parameters of the PID controller by which the controlled quadrotor is stabilized.

Figure 1: A parallel linked quadrotor.

1. Introduction

The development of a quadrotor has been drastically evolved over the last decade. Since its structure is simple and it has high mobility, maintainability, and inexpensiveness, it has been utilized in many fields such as the surveillance and the exploration of disasters (such as a fire, an earthquake, and a flood), and periodic inspection of bridges and tunnels[1, 2].

We consider the case of the inspection of a bridge or a tunnel. Then, the quadrotor observes both its lateral and upward direction. Usually, the camera is attached on the bottom of the quadrotor. So, it is easy to observe its lateral direction, but it is difficult to observe its upward direction because the camera cannot turn to upward. If we attach the camera on the upward of the quadrotor, it is difficult to observe the downward. Moreover, we cannot control the attitude and translational motion of the quadrotor independently because it is an underactuated mechanical system. In other words, a quadrotor has 6 degrees of freedom (3 dimensional translational motions and 3 dimensional attitude rotations) with only 4 degrees of freedom control inputs (the thrust, roll input, pitch input, and yaw input).

Many approaches to the increase of the degrees of its freedom have been studied [3, 4, 5]. M. Ryll et al. developed a quadrotor that has 6 degrees of freedom. They realized that the mounting frame of the rotor that is able to tilt, and the quadrotor has 8 inputs. [6, 7]. However, it is impossible to tilt the quadrotor largely enough to observe the upward. A. Oosedo et al. developed a quadrotor that can change the pitch angle at hovering from 0 to 90 degrees by further increasing the angle of tilt [3]. P. Segui-Gasco et al. developed a quadrotor that has the 8 inputs. By doing so, it does not fall immediately even if one of the rotor is broken [8]. K. Kawasaki et al. developed an H-shaped quadrotor. It can carry out the rotation of the pitch angle of 360 degrees. It needs two additional servo motors for tilting [9].

In this paper, we develop a novel quadrotor that named a parallel linked quadrotor shown in Fig. 1. We utilize a parallel link at the frame of the x-axis direction, and install one servo motor at the center of the quadrotor so that its pitch angle can move from -90 degree to 90 degree. We call this angle a tilt angle. An advantage of this novel quadrotor is that it can hover on the spot in any tilt angle just by using one servo motor. On the other hand, the previous studies used two or more servo motors. Thus, the developed quadrotor has ease of maintenance. In Section 2, we derive the model of developed quadrotor. In Section 3, we consider a PID controller for the stabilization of the developed quadrotor at a specified hovering state. And we investigate gain parameters of the PID controller by which the controlled quadrotor is stabilized. Finally, Section 4 concludes the paper.

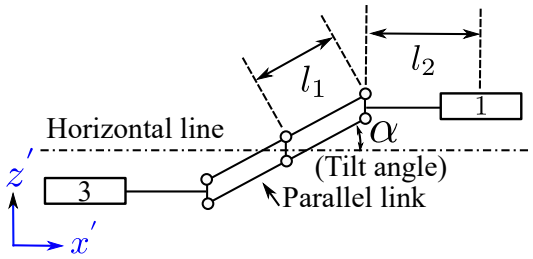

Figure 2: Description of alpha angle.

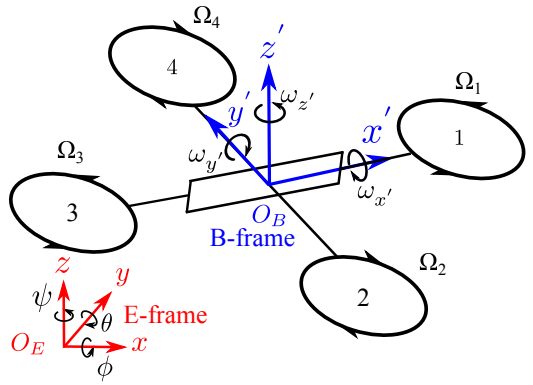

Figure 3: The parallel linked quadrotor coordinate systems with the B-frame and the E-frame.

2. The Parallel Linked Quadrotor

2.1. Features of the Parallel Linked Quadrotor

Shown in Fig. 1 is a developed quadrotor whose propellers tilt by using a parallel link, which will be called a parallel linked quadrotor. As shown in Fig. 2, the developed quadrotor can hover while maintaining a tilting state. Because the parallel link is installed at the x' axis, the rotor can keep the holizontal state. The quadrotor without tilting propellers has only 4 independent control inputs, and has 6-dimensional outputs. In other words, it is impossible to satisfy a desired position and a desired rotation at the same time. However, the developed quadrotor can hover at any pitch angle by changing the tilt angle.

2.2. Modeling of parallel linked quadrotor

In this section, we derive a model of the developed quadrotor. The basic flight control principle is the same as the conventional quadrotor. Fig. 3 shows the configuration frame systems of the developed quadrotor. To describe motions of its rigid body, we introduce the earth inertial reference frame (E-frame) and the body-fixed reference frame (B-frame). The E-frame (O_E, x, y, z) is chosen as the inertial right-hand reference. The B-frame (O_B, x', y', z') is attached to the body. In the following, we impose the following two assumptions. (1)The origin of the B-frame coincides with the center of gravity of the quadrotor. (2)The coordinate axes of the B-frame coincides with the axis of the inertia of the body. As shown in Fig. 3, each propeller from the front in a clockwise is named the numbers 1 to 4. The propellers 1 and 3 rotate the counter-clockwise while the propellers 2 and 4 rotate the clockwise. They produce thrust power by rotating all propellers. The rotational movements of the quadrotor are called roll, pitch, and yaw respectively. Roll is rotational motion around the x' axis of the quadrotor. In the same way, pitch and yaw are rotational motions around the y' and the z' axis of the quadrotor, respectively. In addition to these general rotational movements, we introduce a tilt angle α in the developed quadrotor as shown in Fig. 2. This angle moves by only one servo motor. On the other hand, the thrust and the anti-torque of each rotor are known to be proportional to the square of the rotational speed of the motor. Since the direction of the rotation of the propellers 1 and 3 is opposite to that of the propellers 2 and 4, the corresponding anti-torques generated by the propellers are also in the opposite directions. The thrust T_i and the anti-torque of each rotor Q_i are described by the following equations.

$$T_i = b\Omega_i^2, \quad (1)$$
$$Q_i = (-1)^i d\Omega_i^2, \quad (2)$$

where $i = 1,2,3,4$ are propellers' numbers, b is a thrust constant, and d is an anti-torque constant. Each propeller is driven by a motor, and the thrusts T_i are generated by the propeller rotations. In the quadrotor model, we consider the total thrust U_1[N] and the torque around each axis of the body coordinate system U_2, U_3, and U_4[Nm] as inputs, which are described by the following equations. They are roll, pitch, and yaw input, respectively.

$$U_1 = b(\Omega_1^2 + \Omega_2^2 + \Omega_3^2 + \Omega_4^2), \quad (3)$$
$$U_2 = lb(-\Omega_2^2 + \Omega_4^2), \quad (4)$$
$$U_3 = (l_1 \cos\alpha + l_2)b(-\Omega_1^2 + \Omega_3^2), \quad (5)$$
$$U_4 = d(-\Omega_1^2 + \Omega_2^2 - \Omega_3^2 + \Omega_4^2), \quad (6)$$

where l_1 and l_2 are the lengths of the arms as shown in Fig. 2. From (5), the tilt angle α has an effect on the pitch input U_3 only.

$\boldsymbol{\Gamma_E} = [x\ y\ z]^T$ and $\boldsymbol{\Theta_E} = [\phi\ \theta\ \psi]^T$ denote a position vector of the center of gravity and an altitude angle vector in the E-frame, respectively. ϕ, θ, and ψ are called a roll, a pitch, and a yaw angle, respectively. $\boldsymbol{V_B} = [v_{x'}\ v_{y'}\ v_{z'}]^T$ and $\boldsymbol{\omega_B} = [\omega_{x'}\ \omega_{y'}\ \omega_{z'}]^T$ denote a velocity vector and an angular velocity vector in the B-frame, respectively. The kinematics of the developed quadrotor is described as follows.

$$\dot{\boldsymbol{\Gamma}}_{\boldsymbol{E}} = \boldsymbol{R}\boldsymbol{V_B}, \quad (7)$$
$$\dot{\boldsymbol{\Theta}}_{\boldsymbol{E}} = \boldsymbol{T}\boldsymbol{\omega_B}, \quad (8)$$

where $\boldsymbol{R}$ is a rotation matrix and $\boldsymbol{T}$ is a transfer matrix given by

$$\boldsymbol{R} = \begin{bmatrix} c_\psi c_\theta & -s_\psi c_\phi + c_\psi s_\theta s_\phi & s_\psi s_\phi + c_\psi s_\theta c_\phi \\ s_\psi c_\theta & c_\psi c_\phi + s_\psi s_\theta s_\phi & -c_\psi s_\phi + s_\psi s_\theta c_\phi \\ -s_\theta & c_\theta s_\phi & c_\theta c_\phi \end{bmatrix}, \quad (9)$$

Table 1: Specifications of the parallel linked quadrotor.

	Value		Value
m	1.46[kg]	Jz_0	6.83×10^{-3}[kg m^2]
l_1	0.220[m]	Jx_{45}	4.11×10^{-3}[kg m^2]
l_2	0.165[m]	Jy_{45}	5.20×10^{-3}[kg m^2]
l	l_1+l_2[m]	Jz_{45}	4.83×10^{-3}[kg m^2]
Jm	2.06×10^{-6}[kg m^2]	Jx_{90}	5.74×10^{-3}[kg m^2]
Jx_0	2.41×10^{-3}[kg m^2]	Jy_{90}	4.51×10^{-3}[kg m^2]
Jy_0	5.49×10^{-3}[kg m^2]	Jz_{90}	2.51×10^{-3}[kg m^2]

$$\boldsymbol{T} = \begin{bmatrix} 1 & s_\phi t_\theta & c_\phi t_\theta \\ 0 & c_\phi & -s_\phi \\ 0 & s_\phi/c_\theta & c_\phi/c_\theta \end{bmatrix}, \tag{10}$$

and $s_j = \sin j$, $c_j = \cos j$, $t_j = \tan j$ ($j = \phi,\ \theta,\ \psi.$). Thus, the quadrotor is modeled by the following equation.

$$\begin{bmatrix} m\boldsymbol{I}_{3\times3} & \boldsymbol{0}_{3\times3} \\ \boldsymbol{0}_{3\times3} & \boldsymbol{J}(\alpha) \end{bmatrix} \begin{bmatrix} \dot{\boldsymbol{V}}_{\boldsymbol{B}} \\ \dot{\boldsymbol{\omega}}_{\boldsymbol{B}} \end{bmatrix} + \begin{bmatrix} \boldsymbol{\omega}_{\boldsymbol{B}} \times (m\boldsymbol{V}_{\boldsymbol{B}}) \\ \boldsymbol{\omega}_{\boldsymbol{B}} \times (\boldsymbol{J}(\alpha)\boldsymbol{\omega}_{\boldsymbol{B}}) \end{bmatrix} = \begin{bmatrix} \boldsymbol{F}_{\boldsymbol{B}} \\ \boldsymbol{\tau}_{\boldsymbol{B}} \end{bmatrix}, \tag{11}$$

where $\boldsymbol{I}$ is the unit matrix, $\boldsymbol{J}(\alpha) = [J_x(\alpha)\ J_y(\alpha)\ J_z(\alpha)]^T$ is an inertia matrix of the developed quadrotor, and m is its mass. When the tilt angle α changes, the shape of the developed quadrotor is also changed. Thus, the inertias depend on the tilt angle. The second term in the left-hand side is the Coriolis force acting on the apparent in B-frame. Besides, the translational motion is modeled by the E-frame. Its right-hand side represents forces and torques acting to the quadrotor. Concretely speaking, they represent gyro effects generated by the propeller rotations, the gravity force applied to the body, thrust forces and torques of propellers' rotations. In addition, the anti-torque is generated by tilting movement. This term appears in the pitch equation. Here, we can translate $\boldsymbol{\omega}_{\boldsymbol{B}}$ to $\boldsymbol{\Theta}_{\boldsymbol{E}}$ by using the transfer matrix $\boldsymbol{T}$. However, since we consider the situation of hovering, the attitude angle is close to zero. Thus a transfer matrix can be approximated to the unit matrix. In other words, we can replace $\boldsymbol{\omega}_{\boldsymbol{B}}$ with $\boldsymbol{\Theta}_{\boldsymbol{E}}$. Then, we can neglect the effect of air resistance generated by the translational motion. Under these assumptions, (11) is rewritten as follows.

$$\begin{cases} \ddot{x} = a_x \frac{U_1}{m}, \\ \ddot{y} = a_y \frac{U_1}{m}, \\ \ddot{z} = -g + a_z \frac{U_1}{m}, \\ \ddot{\phi} = \frac{J_y(\alpha)-J_z(\alpha)}{J_x(\alpha)}\dot{\theta}\dot{\psi} - \frac{J_m}{J_x(\alpha)}\dot{\theta}\Omega + \frac{U_2}{J_x(\alpha)}, \\ \ddot{\theta} = \frac{J_z(\alpha)-J_x(\alpha)}{J_y}\dot{\phi}\dot{\psi} - \frac{J_m}{J_y(\alpha)}\dot{\phi}\Omega + \frac{U_3}{J_y(\alpha)} - \ddot{\alpha}, \\ \ddot{\psi} = \frac{J_x(\alpha)-J_y(\alpha)}{J_z(\alpha)}\dot{\phi}\dot{\theta} + \frac{U_4}{J_z(\alpha)}, \end{cases} \tag{12}$$

where $a_x = (s_\psi s_\phi + c_\psi s_\theta c_\phi)$, $a_y = (-c_\psi s_\phi + s_\psi s_\theta c_\phi)$, $a_z = (c_\theta c_\phi)$, J_m is a motor inertia, and $\Omega = \Omega_1 + \Omega_2 + \Omega_3 + \Omega_4$.

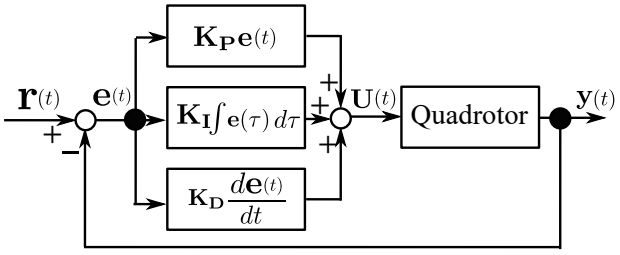

Figure 4: A block diagram of PID control.

Table 2: Nominal gains of the PID controller.

	Gain		Gain
K_{Pz}	100	$K_{P\theta}$	10
K_{Iz}	50	$K_{I\theta}$	10
K_{Dz}	50	$K_{D\theta}$	1
$K_{P\phi}$	10	$K_{P\psi}$	10
$K_{I\phi}$	10	$K_{I\psi}$	10
$K_{Dz\phi}$	1	$K_{D\psi}$	1

3. PID control

In this section, we consider PID control for the stabilization of the developed quadrotor at the hovering state. Fig. 4 shows a block diagram of the PID controller, where $\mathbf{r}(t) = [z_m\ 0\ 0\ \psi_m]^T$, $\mathbf{e}(t) = \mathbf{r}(t) - \mathbf{y}(t)$, $\mathbf{U}(t) = [U_1\ U_2\ U_3\ U_4]^T$, $\mathbf{y}(t) = [z\ \phi\ \theta\ \psi]^T$, $\mathbf{K_P} = diag[K_{PZ}\ K_{P\phi}\ K_{P\theta}\ K_{P\psi}]$, $\mathbf{K_I} = diag[K_{IZ}\ K_{I\phi}\ K_{I\theta}\ K_{I\psi}]$, and $\mathbf{K_D} = diag[K_{DZ}\ K_{D\phi}\ K_{D\theta}\ K_{D\psi}]$. Since we use the PID controller, the target state is an equilibrium point of the controlled quadrotor, that is, the equilibrium point are given by $z = z_m$, $\psi = \psi_m$, $\dot{z} = \phi = \dot{\phi} = \theta = \dot{\theta} = \dot{\psi} = 0$. We consider the linearized system of the controlled quadrotor around the equilibrium point. The parameters of the developed quadrotor are given in Table 1. And nominal gains of the controller are listed in Table 2. Shown in Figs. 5 and 6 are boundaries of the stability regions on the $K_{D\phi} - K_{P\phi}$ and the $K_{D\psi} - K_{P\psi}$ parameter plane, respectively, when the tilt angle is changed, where the other gains are fixed to the nominal values. The region above the boundary is a stability region. From these figures, it is shown that, as the tilt angle increases, we have to increase the gains for pitch $K_{D\phi}$ and $K_{P\phi}$ while we can decrease those for yaw $K_{D\psi}$ and $K_{P\psi}$. Because, by the increase of the tilt angle, J_x increases while J_z decreases. Fig. 7 shows the behavior of the mathematical model when the initial value of roll angle is 0.2[rad] (= 11.5[deg]).

4. Conclusion

In this paper, we developed a novel quadrotor named the parallel linked quadrotor, where tilting is realized by a parallel link and one servo motor. We derived a model of the quadrotor. We consider PID control for the stabilization of its hovering state. We investigated stabilization regions on gain parameter planes. It was shown that, as the tilt an-

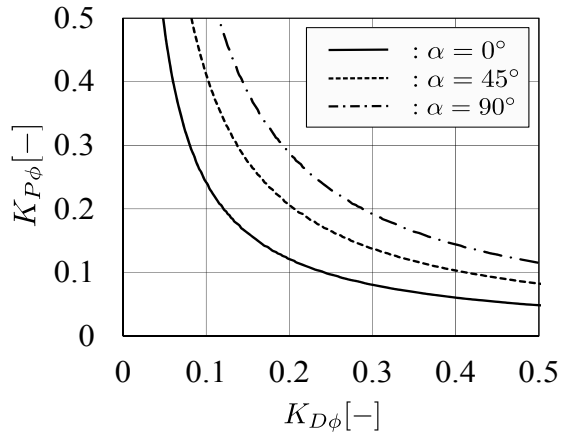

Figure 5: Stabilization region on the $K_{D\phi} - K_{P\phi}$ plane.

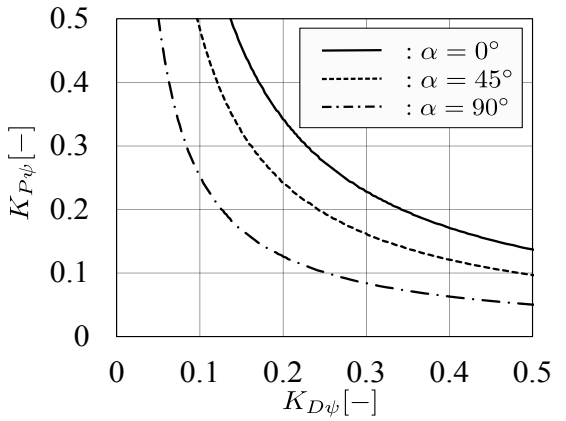

Figure 6: Stabilization region on the $K_{D\psi} - K_{P\psi}$ plane.

gle increases, we have to increase the gains for pitch while we can decrease those for yaw. Because, by the increase of the tilt angle, J_x increases while J_z decreases. The experiment by a prototype of the quadrotor is future work. It is also future work to investigate an effect of the anti-torque generated by the servo motor on the pitch rotation.

Acknowledgments This research was supported in part by JSPS KAKENHI Grant Number JP24656262.

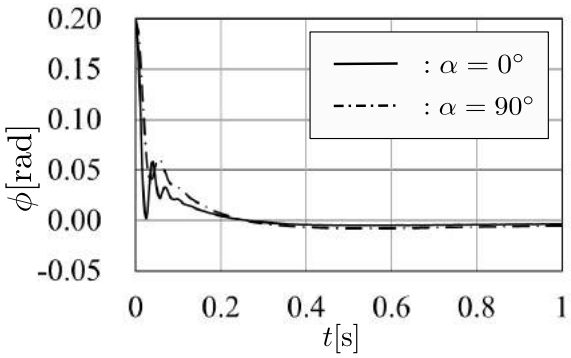

Figure 7: Time response of the roll angle.

References

[1] N. Michael et al, "Collaborative mapping of an earthquake-damaged building via ground and aerial robots", *Journal of Field Robotics*, vol. 29, no. 5, pp. 832-841, 2012.

[2] N. Metni, and T. Hamel, "A UAV for bridge inspection: Visual servoing control law with orientation limits", *Automation in Construction*, Vol. 17, no. 1, pp. 3-10, 2007.

[3] A. Oosedo, S. Abiko, S. Narasakiand, A. Kuno, A. Konno, and M. Uchiyama, "Flight control systems of a quad tilt rotor unmanned aerial vehicle for a large attitude change", *in Proc. IEEE Int. Conf. on Robotics and Automation*, pp. 2326-2331, 2015.

[4] A. Nemati and M. Kumar, "Modeling and control of a single axis tilting quadcopter", *in Proc. IEEE American Control Conf*, pp. 3077-3082, 2014.

[5] C. Hintz, T. Cody, and L. R. G. Carrillo, "Design and dynamic modeling of a rotary wing aircraft with morphing capabilities", *in Proc. IEEE Int. Conf. on Unmanned Aircraft Systems*, pp. 492-498, 2014.

[6] M. Ryll, H. H. Bulthoff, and P. R. Giordano, "Modeling and control of a quadrotor UAV with tilting propeller", *in Proc. IEEE Int. Conf. on Robotics and Automation*, pp. 4606-4613, 2012.

[7] M. Ryll, H. H. Bulthoff, and P. R. Giordano, "First flight tests for a quadrotor UAV with tilting propeller", *in Proc. IEEE Int. Conf. on Robotics and Automation*, pp. 295-302, 2013.

[8] P. S. Gasco, Y. A. Rihani, H. S. Shin, and A. Savvaris, "A novel actuation concept for a multi rotor UAV", *Journal of Intelligent and Robotic Systems*, Vol. 74, no. 1-2, pp. 173-191, 2014.

[9] K. Kawasaki, Y. Motegi, M, Zhao, K. Okada, and M. Inaba, "Dual connected bi-copter with new wall trace locomotion feasibility that can fly at arbitrary tilt angle", *in Proc IEEE/RSJ Int. Conf. on Intelligent Robots and Systems*, pp. 524-531. 2015.

[10] S. Bouabdallah and R. Siegwart, "Backstepping and sliding-mode techniques applied to an indoor micro quadrotor", *in Proc. IEEE Int. Conf. on Robotics and Automation*, pp. 2247-2252, 2005.

[11] S. Bouabdallah, P. Murrieriand and R. Siegwart, "Towards autonomous indoor micro VTOL", *Autonomous robots*, Vol. 18, no 2, pp. 171-183, 2005.